ChemComm

Cite this: *Chem. Commun.*, 2011, **47**, 6168–6170

www.rsc.org/chemcomm

COMMUNICATION

Highly chemoselective hydrogenation of crotonaldehyde over Ag–In/SBA-15 fabricated by a modified "two solvents" strategy

Li Tian,[a] Qiuyun Yang,[a] Zheng Jiang,[b] Yuan Zhu,[a] Yan Pei,*[a] Minghua Qiao*[a] and Kangnian Fan[a]

Received 21st February 2011, Accepted 2nd April 2011
DOI: 10.1039/c1cc11013f

In the challenging crotonaldehyde hydrogenation to crotyl alcohol, an Ag–In/SBA-15 catalyst fabricated by a modified "two solvents" strategy shows an unprecedentedly high yield of 86% at a selectivity of 87%, which exceeds the best results on Pt-, Au- and other Ag-based heterogeneous catalysts reported so far.

Among α,β-unsaturated aldehydes, crotonaldehyde (CRAL) is one of the most difficult molecules to be selectively hydrogenated to α,β-unsaturated alcohols over heterogeneous catalysts. However, Ag, a well-documented oxidation catalyst, unexpectedly exhibits notably high selectivity in CRAL hydrogenation to crotyl alcohol (CROL).[1,2] Unlike Pt and Au that always rely on promoter and reducible support to evoke their high selectivity, Ag is intrinsically selective in saturating the C=O bond in conjugation with the C=C bond.[2–5] Moreover, Claus and co-workers experimentally,[6,7] and later on Zhang and co-workers theoretically and experimentally[5] demonstrated, that the formation of α,β-unsaturated alcohols is preferred on small Ag nanoparticles (AgNPs).

In the family of mesoporous materials, SBA-15 is one of the most ideal catalyst supports due to its high surface area, high porosity, and large and uniform channel size.[8] These features provide a consistent and well-isolated environment for the growth of nanoparticles, which is of particular interest for size-dependent reactions. Herein, we report the fabrication and characterization of SBA-15-supported Ag and In-promoted Ag catalysts by a modified "two solvents" strategy for CRAL hydrogenation to CROL. The usual "two solvents" strategy is based on a volume of the metal salt aqueous solution set equal to the pore volume of SBA-15. The introduction of the metal salt into the hydrophilic channels of SBA-15 is driven by the capillary force in the presence of an organic solvent.[9–11] In this approach, several regular metal oxide nanostructures have been fabricated successfully. We modified this strategy by using an excess volume of aqueous solution, since our preliminary experiments revealed a poor catalytic performance of the Ag/SBA-15 catalyst prepared following the usual "two solvents" strategy.

Table 1 Physicochemical properties of the Ag/SBA-15 and Ag–In/SBA-15 catalysts fabricated by the modified "two solvents" strategy

Catalyst	Loading (wt%)		Ag/Si[a] (%)	S_{BET}/ $m^2 g^{-1}$	V_{pore}/ $cm^3 g^{-1}$	d_{pore}/ nm
	Ag	In				
SBA-15	—	—	—	750	1.02	6.9
Ag/SBA-15	6.9	—	4.2	582	1.09	6.7
Ag–In/SBA-15	6.1	1.9	4.6	496	0.91	6.6

[a] Surface atomic ratio determined by XPS.

Siliceous mesoporous SBA-15 was synthesized according to the published procedures.[8] Then, 1.0 g of the calcined SBA-15 was homogeneously dispersed in 50 ml of cyclohexane under vigorous stirring at room temperature. Following this, 5.0 ml of the $AgNO_3$ aqueous solution was added dropwise into the dispersion. The nominal Ag loading relative to SBA-15 was 9.0 wt%. The slurry was evaporated to dryness at 343 K and heated at 373 K overnight. The resulting solids were calcined at 623 K for 4 h and reduced in a 5 vol% H_2/Ar flow at 573 K for 4 h. The as-fabricated catalyst is designated Ag/SBA-15. The Ag–In/SBA-15 catalyst was similarly fabricated, except that the aqueous solution contained both $AgNO_3$ and $In(NO_3)_3$. The nominal Ag and In loadings relative to SBA-15 in this catalyst were 9.0 and 3.0 wt%, respectively. The practical loadings and textural properties of these catalysts are summarized in Table 1.

Fig. 1a presents transmission electron micrographs (TEM; JEOL JEM2011) of the Ag/SBA-15 catalyst fabricated by the modified "two solvents" strategy. It shows that the AgNPs are dispersed evenly inside the entire SBA-15 host instead of on the exterior, as most AgNPs are located between two immediate neighboring channel walls. The mean particle size of the AgNPs is 6.1 ± 1.3 nm. The decreased BET surface area and pore volume of Ag/SBA-15 in comparison to SBA-15 (Table 1) substantiate the encapsulation of the AgNPs in the channels of SBA-15. Early methods for the fabrication of SBA-15-supported AgNPs can be mainly classified into three categories: (1) wetness impregnation of SBA-15 with silver salt,[12] (2) synthesis of SBA-15 in the coexistence of silver salt and chemical reductant,[13] and (3) synthesis of SBA-15 in the presence of pre-formed AgNPs.[14] However, the former two methods inevitably produce large Ag particles or aggregates on the external surface, while the

---

[a] *Department of Chemistry and Shanghai Key Laboratory of Molecular Catalysis and Innovative Materials, Fudan University, Shanghai, 200433, P. R. China. E-mail: mhqiao@fudan.edu.cn, peiyan@fudan.edu.cn; Fax: +86 21 6564 1740; Tel: +86 21 55664679*
[b] *Shanghai Synchrotron Radiation Facility, Shanghai Institute of Applied Physics, Chinese Academy of Sciences, Shanghai 201204, P.R. China*

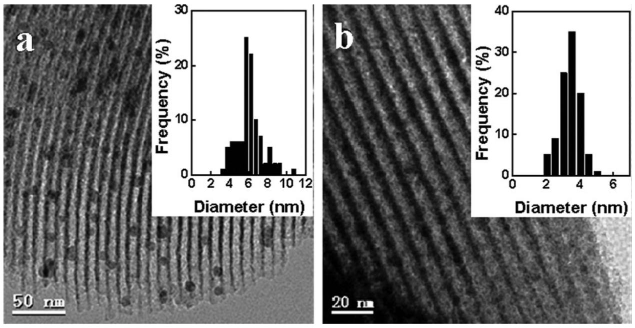

Fig. 1 TEM images and particle size distribution histograms (insets) of (a) Ag/SBA-15 and (b) Ag–In/SBA-15 fabricated by the modified "two solvents" strategy recorded along the [110] zone axis of SBA-15.

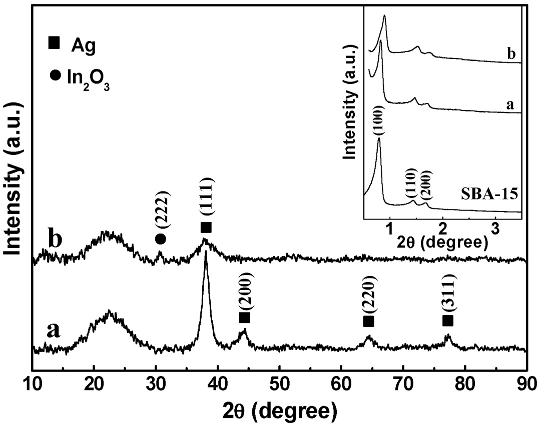

Fig. 2 Wide- and small-angle (inset) XRD patterns of (a) Ag/SBA-15 and (b) Ag–In/SBA-15 fabricated by the modified "two solvents" strategy.

last method involves complicated pre-synthesis of size-controlled AgNPs and rigorous encapsulation steps. The modified "two solvents" strategy is thus advantageous relative to those methods in its convenience and effectiveness.

Surprisingly, when the same strategy was used to fabricate the Ag–In/SBA-15 catalyst, the AgNPs could hardly be discerned in the low-magnification image as Fig. 1a, although more metal was loaded in this case (see Table 1). Only in the TEM image with higher magnification the AgNPs of 3.4 ± 0.6 nm adhering to the channel walls of SBA-15 were identified (Fig. 1b), suggesting that In is efficient in further dispersing the AgNPs. This observation is corroborated by the distinct difference between their wide-angle X-ray diffraction patterns (XRD; Bruker AXS D8 Advance). For Ag/SBA-15, besides the broad peak at $2\theta \approx 22°$ due to amorphous silica, there are pronounced diffraction peaks attributable to fcc Ag (JCPDS 04-0783) (Fig. 2). For Ag–In/SBA-15, the diffractions of Ag are attenuated markedly, leaving only the once strongest Ag(111) peak that now becomes weak and broad. The assignment of this peak to fcc Ag is validated by the identical Ag K-edge X-ray absorption spectra (XAS; SSRF) of Ag–In/SBA-15 and Ag/SBA-15 (Fig. 3). It is known that for Ag metal, the intensity of the whiteline (first continuum resonance) in the Ag K-edge spectrum is nearly the same as that of the adjacent resonances. Based on the Scherrer equation, the Ag crystallite sizes perpendicular to the {111} planes were estimated as 6.4 and 2.7 nm for Ag/SBA-15 and Ag–In/SBA-15, respectively, falling well in the ranges of the particle sizes measured by TEM.

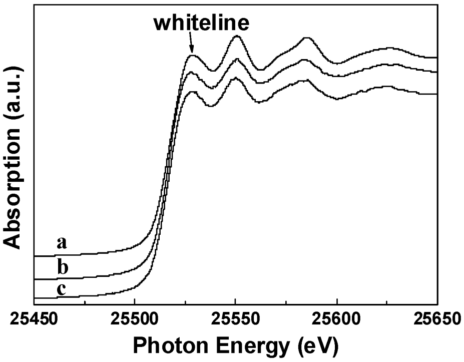

Fig. 3 Ag K-edge XAS spectra of (a) Ag foil, (b) Ag/SBA-15 and (c) Ag–In/SBA-15 fabricated by the modified "two solvents" strategy.

Table 2 Hydrogenation results over the Ag/SBA-15 and Ag–In/SBA-15 catalysts fabricated by the modified "two solvents" strategy[a]

			Selectivity[b] (%)				
Catalyst	t^b/min	Conv.[b] (%)	CROL	BUAL[d]	BUOL[e]	Y^b (%)	r_0^c
Ag/SBA-15	245	95	54	21	25	51	391
Ag–In/SBA-15	740	99	87	3	10	86	283

[a] *Reaction conditions*: 0.2 g catalyst, 0.1 ml CRAL, 29 ml *n*-hexane, reaction temperature 413 K, H_2 pressure 2.0 MPa, and stirring rate 1000 rpm. [b] Values corresponding to the maximum yield of CROL. [c] Initial hydrogenation rate in μmol min^{-1} $g_{Ag}{}^{-1}$. [d] BUAL: butanal. [e] BUOL: butanol.

In Fig. 2, there is an additional small peak at 2θ of 30.6° for Ag–In/SBA-15. This feature is assigned to the (222) reflection of In_2O_3 (JCPDS 06-0416), since when we further increased the loading of In, this feature was intensified, along with the appearance of other peaks relating to In_2O_3. The inset in Fig. 2 confirms again that the mesoscopic ordering of SBA-15 was retained in both catalysts fabricated by the modified "two solvents" strategy, with the clear observation of all three small-angle peaks characteristic of the hexagonal mesostructure of SBA-15.

Table 2 compiles the catalytic results over the Ag/SBA-15 and Ag–In/SBA-15 catalysts fabricated by the modified "two solvents" strategy in liquid-phase hydrogenation of CRAL. Consistent with previous work on selective hydrogenation of acrolein[15] and citral on Ag catalysts,[16] In is remarkable in improving the selectivity to α,β-unsaturated alcohol. On the Ag–In/SBA-15 catalyst prepared by the modified "two solvents" strategy, the maximum yield of CROL was drastically increased to 86% with the corresponding selectivity as high as 87%, as compared to the yield of 51% and the selectivity of 54% on the Ag/SBA-15 catalyst (Table 2). It is worth emphasizing here that the CROL yield on the present Ag–In/SBA-15 catalyst excels the best values on literature Pt-, Au- and Ag-based catalysts *via* catalytic hydrogenation. For example, the highest CROL yield reported so far was 71% obtained on an $Au_{5.0}In_{0.75}$/APTMS-SBA-15 catalyst.[17] The most selective Ag-based catalyst ever reported is the Ag–$MnO_2/Al_2O_3{\cdot}5AlPO_4$ catalyst developed by Nagase *et al.*,[1] on which a CROL yield of 69.5% was obtained under more stringent reaction conditions (reaction temperature 423 K, H_2 pressure 5 MPa) than ours.

It is acknowledged that the chemisorption mode of the substrate is decisive to the selectivity in the hydrogenation of α,β-unsaturated aldehydes.[18] The preferential binding through the C=O bond, *e.g.*, the η_1-on-top mode *via* the terminal oxygen atom, should favor a high selectivity to α,β-unsaturated alcohols. Based on density functional theory, it is found that while the adsorption of CRAL on the Ag(111) surface is negligible, the energetically most favored adsorption mode on an Ag_{19} cluster with fcc structure is the η_1-on-top mode bound on coordinatively unsaturated Ag atoms.[5] Likewise, Fujii *et al.* found that acrolein can coordinate through the C=O bond to the positively charged sites (probably ad-adatom and/or kink sites) on an evaporated Ag film.[19] Alternatively, the positively charged Ag sites may arise from electronic modification by subsurface oxygen in Ag formed during the process of catalyst preparation or hydrogenation. These sites are more abundant on supported Ag than on unsupported polycrystalline Ag.[7] Both interpretations point to a higher selectivity to α,β-unsaturated alcohols on smaller AgNPs, since the abundance of either the coordinatively unsaturated or the positively charged Ag sites is inversely proportional to the Ag particle size. This idea was validated by Zhang and co-workers on Ag/SiO_2 catalysts with Ag particle sizes ranging from 4.8 to >11.3 nm for CRAL hydrogenation[5] and by Claus and co-workers on Ag(111) and (100) single crystals, sputtered Ag, and Ag/SiO_2 prepared by three different methods for acrolein hydrogenation.[6] Such a size effect may operate on the Ag/SBA-15 and Ag–In/SBA-15 catalysts, which is reflected in the much higher CROL selectivity on the Ag–In/SBA-15 catalyst with much smaller AgNPs.

However, the selectivity enhancement is not exclusively limited to the size effect of Ag. Claus and Hofmeister reported a CROL selectivity of only 57% on an Ag/SiO_2 catalyst with an average particle size of 3.7 nm.[2] Although the reaction conditions are in variance with ours, such a distinctive selectivity difference between their catalyst and our Ag–In/SBA-15 catalyst with similar Ag particle size clearly indicates that In_2O_3 plays an important role in improving CROL selectivity. The involvement of In_2O_3 in CRAL hydrogenation is evidenced by the lower hydrogenation rate on Ag–In/SBA-15 than on Ag/SBA-15 (Table 2), or smaller AgNPs would have led to a higher rate.[7] This activity loss infers that the AgNPs were decorated by In_2O_3, thus blocking some Ag sites. Because of the inclusion of the AgNPs in the channels and the amorphous nature of SBA-15, it is impossible to directly observe the decoration of the AgNPs by In_2O_3 by high-resolution TEM. However, X-ray photoelectron spectroscopy (XPS; Perkin Elmer PHI5000C) revealed an Ag/Si surface atomic ratio of 4.6% for Ag–In/SBA-15, which is only slightly higher than the ratio of 4.2% for Ag/SBA-15 (Table 1). Assuming that the presence of In_2O_3 and the improved dispersion of Ag do not alter the surface exposure of SBA-15, a simple calculation shows that the Ag/Si surface ratio on Ag–In/SBA-15 should be at least 1.6 times of that on Ag/SBA-15, if the surface of the AgNPs was In_2O_3-free. In light of these facts, we propose that a portion of In_2O_3 covered the AgNPs. Metal oxides, including In_2O_3, can function as Lewis acid sites, which aid in the adsorption and activation of the C=O bond *via* the electron lone pair on oxygen.[7] This may be another important reason underlying the unprecedentedly high selectivity to CROL on the Ag–In/SBA-15 catalyst.

In summary, the Ag–In/SBA-15 catalyst prepared by the modified "two solvents" strategy is highly selective in the challenging CRAL hydrogenation to CROL. Its excellent catalytic performance is attributed to the combined effects of the reduced AgNPs bearing a high population of the coordinatively unsaturated or positively charged Ag sites and the presence of In_2O_3 functioning as Lewis acid sites, both favoring the adsorption and activation of the C=O bond in CRAL. The present work, together with our previous work on SBA-15-supported Ru-based catalysts prepared by the same strategy,[20,21] shows the prospect of the modified "two solvents" strategy as a routine and effective method for the fabrication of highly dispersed metal nanocrystals accommodated in mesoporous materials with improved catalytic performances.

Financial support from the NSF of China (20803011, 21073043), the Shanghai Science and Technology Committee (10JC1401800, 08DZ2270500), and the Program of New Century Excellent Talents in Universities (NCET-08-0126) is gratefully acknowledged.

Notes and references

1 Y. Nagase, H. Muramatu and T. Satō, *Chem. Lett.*, 1988, 1695.
2 P. Claus and H. Hofmeister, *J. Phys. Chem. B*, 1999, **103**, 2766.
3 P. G. N. Mertens, F. Guypers, P. Vandezande, X. P. Ye, F. Verpoort, I. F. J. Vankelecom and D. E. De Vos, *Appl. Catal., A*, 2007, **325**, 130.
4 C. E. Volckmar, M. Bron, U. Bentrup, A. Martin and P. Claus, *J. Catal.*, 2009, **261**, 1.
5 X. F. Yang, A. Q. Wang, X. D. Wang, T. Zhang, K. L. Han and J. Li, *J. Phys. Chem. C*, 2009, **113**, 20918.
6 M. Bron, D. Teschner, A. Knop-Gericke, B. Steinhauer, A. Scheybal, M. Hävecker, D. Wang, R. Födisch, D. Hönicke, A. Wootsch, R. Schlögl and P. Claus, *J. Catal.*, 2005, **234**, 37.
7 M. Bron, D. Teschner, A. Knop-Gericke, F. C. Jentoft, J. Kröhnert, J. Hohmeyer, C. Volckmar, B. Steinhauer, R. Schlögl and P. Claus, *Phys. Chem. Chem. Phys.*, 2007, **9**, 3559.
8 D. Y. Zhao, J. L. Feng, Q. S. Huo, N. Melosh, G. H. Fredrickson, B. F. Chmelka and G. D. Stucky, *Science*, 1998, **279**, 548.
9 M. I. Clerc, D. Bazin, M. D. Appay, P. Beaunier and A. Davidson, *Chem. Mater.*, 2004, **16**, 1813.
10 I. Lopes, N. El Hassan, H. Guerba, G. Wallez and A. Davidson, *Chem. Mater.*, 2006, **18**, 5826.
11 Q. S. Lu, Z. Y. Wang, J. G. Li, P. Y. Wang and X. L. Ye, *Nanoscale Res. Lett.*, 2009, **4**, 646.
12 M. Boutros, J. M. Trichard and P. Da Costa, *Appl. Catal., B*, 2009, **91**, 640.
13 D. Tian, G. P. Yong, Y. Dai, X. Y. Yan and S. M. Liu, *Catal. Lett.*, 2009, **130**, 211.
14 J. Zhu, Z. Kónya, V. F. Puntes, I. Kiricsi, C. X. Miao, J. W. Ager, A. P. Alivisatos and G. A. Somorjai, *Langmuir*, 2003, **19**, 4396.
15 M. Lucas and P. Claus, *Chem. Eng. Technol.*, 2005, **28**, 867.
16 M. Steffan, M. Lucas, A. Brandner, M. Wollny, M. Oldenburg and P. Claus, *Chem. Eng. Technol.*, 2007, **30**, 481.
17 Q. Y. Yang, Y. Zhu, L. Tian, S. H. Xie, Y. Pei, H. Li, H. X. Li, M. H. Qiao and K. N. Fan, *Appl. Catal., A*, 2009, **369**, 67.
18 V. Ponec, *Appl. Catal., A*, 1997, **149**, 27.
19 S. Fujii, N. Osaka, M. Akita and K. Itoh, *J. Phys. Chem.*, 1995, **99**, 6994.
20 J. Bu, J. L. Liu, X. Y. Chen, J. H. Zhuang, S. R. Yan, M. H. Qiao, H. Y. He and K. N. Fan, *Catal. Commun.*, 2008, **9**, 2612.
21 J. L. Liu, L. J. Zhu, Y. Pei, J. H. Zhuang, H. Li, H. X. Li, M. H. Qiao and K. N. Fan, *Appl. Catal., A*, 2009, **353**, 282.